J. Ind. Eng. Chem., **Vol. 13**, No. 6, (2007) 939-943

High Density Plasma Etching of Nickel Thin Films Using a Cl_2/Ar Plasma

Han Na Cho, Su Ryun Min, Hyung Jin Bae*, **Jung Hyun Lee***, **and Chee Won Chung**†

Department of Chemical Engineering, Inha University, Incheon 402-751, Korea
**Nano Fabrication Technology Center, Samsung Advanced Institute of Technology, Yongin, Gyunggi-do 446-712, Korea*

Received March 20, 2007; Accepted July 5, 2007

Abstract: The etch characteristics of Ni thin films masked with a photoresist were investigated using inductively coupled plasma reactive ion etching in a Cl_2/Ar gas mix. As the Cl_2 concentration increased, the etch rate of Ni films decreased and the redeposited materials around the etched films were reduced. These results indicate that the etching of Ni films obeys mainly a physical mechanism. The reduction of redeposited materials with increasing Cl_2 concentration implies the involvement of chemical reaction in the etching of Ni thin films. The degree of etch anisotropy was improved with increasing coil rf power and dc-bias voltage. Slight improvement in the etch profile was observed at low gas pressure. An x-ray photoelectron spectroscopy analysis confirmed the formation of $NiCl_2$ compound on the etched surface. Therefore, it can be concluded that the etching of Ni films is governed by physical sputtering along with the assistance of chemical reaction.

Keywords: *nickel, dry etching, Cl_2/Ar, OxRRAM*

Introduction

Magnetic metals such as NiFe, Ni, and Fe are widely used in data-storage systems, magnetic sensors and actuators, and electrochemical sensors [1-3]. These applications have promoted the study on dry etch process of these materials. Recently, the continuous development of information and communication field requires new memory devices having the abilities of high-density integration and high-speed operation. Nonvolatile resistive memories have been intensively studied as one of new memories which satisfy these requirements. Nickel thin films studied in this paper were used as an electrode in resistance memory and an element of magnetic multilayer in magnetic random access memory. Generally, the resistive memories offer the advantages of low power consumption and low production cost, multi-bit storage, fast access, small cell size, and the possibility of write-erase more than 10^{10} times. In addition, because of simple structure, the cost and defect of the manufacturing process are low. Owing to these advantages, resistive memories are considered to have strong potential for a variety of applications [4,5].

Oxide resistive random access memory (OxRRAM), which is one kind of resistive memories, consists of one transistor and one resistor. Generally, in this OxRRAM memory device, binary oxide diodes such as nickel oxide (NiO), titanium oxide (TiO_2), vanadium oxide (VO_2), niobium oxide (Nb_2O_5), and tantalum oxide (Ta_2O_5) were used as the resistor, and nickel (Ni), titanium (Ti), and titanium nitride (TiN) were used as the electrodes [6]. Among these electrodes, Ni thin films are considered to be a prospective candidate because NiO thin films are known to be best materials as a binary oxide diode and are compatible with Ni films. In order to fabricate OxRRAMs, these metal and metal oxides need to be patterned with fine geometry [7].

Generally, Ni thin films, as a magnetic material, are known to be relatively inert under conventional dry etching processes such as ion milling and reactive ion etching [2,3,8,10]. Ion milling suffers from two drawbacks. One is that redeposition is generated on the sidewalls of the etched films. The other is that the slow etch rates cause

---

† To whom all correspondence should be addressed.
(e-mail: cwchung@inha.ac.kr)

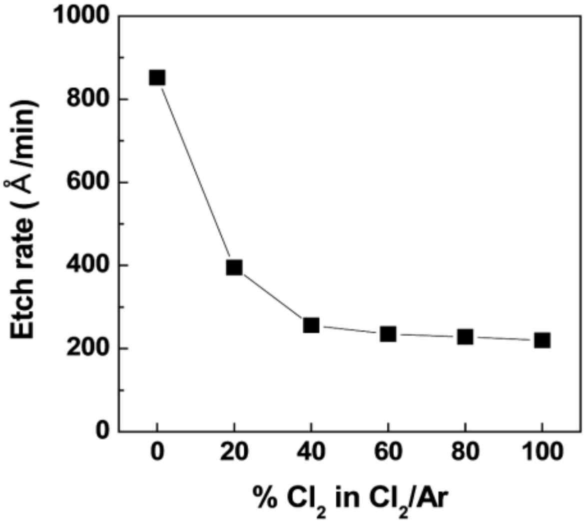

Figure 1. Etch rate of Ni thin films at various Cl_2 concentrations; coil rf power of 700 W, dc-bias voltage of 300 V, gas pressure of 5 mTorr.

low selectivity to the mask and slanted etch profiles. In this study, the etch characteristics of Ni thin films patterned with a photoresist (PR) mask were investigated using inductively coupled plasma reactive ion etching (ICPRIE) in a Cl_2/Ar gas. X-ray photoelectron spectroscopy (XPS) was employed to elucidate the etch mechanism of Ni thin films.

Experimental details

Ni thin films were prepared on a Ti/SiO_2/Si substrate by e-beam evaporation. The films with the thickness of 250 nm were deposited and patterned by conventional lithography. The photoresist mask used was PFI-03A9 and its thickness was 1.2 μm.

In this study, the etching of Ni films was carried out using commercial ICPRIE system (A-Tech, Korea). The ICPRIE system is divided by a main process chamber and a load lock chamber. A coil installed at the top of the main process chamber was connected to a 13.56 MHz rf power supply to generate high density plasma. Self dc-bias voltage induced by rf power at 13.56 MHz was capacitively coupled to the substrate susceptor in order to control the ions' energy in the plasma. The main process chamber was evacuated by a turbomolecular pump to a base pressure of $2 \sim 3 \times 10^{-6}$ Torr. The substrate susceptor was cooled by chilled fluid and held at a constant temperature of 15 °C. The substrate was subsequently cooled via cold helium gas filled between the substrate and susceptor.

A Cl_2/Ar gas mix was used as an etch gas and fed into the main chamber at a rate of 30 sccm. The etch rates and etch profiles of Ni thin films were examined by varying Cl_2 gas concentration. In addition, the effects of etch parameters such as coil rf power, dc-bias voltage, and gas pressure were examined. A surface profilomer (Alpha step, Tencor P-1) was used to measure the etch rates. The etch profiles were observed by field emission scanning electron microscopy (FESEM). XPS was employed to examine the existence of possible etch products on the etched surface. The XPS analysis enabled us to understand the etch mechanism of Ni films in a Cl_2/Ar plasma.

Results and Discussion

Figure 1 showed the etch rate of Ni thin films by varying Cl_2 concentration. The standard etch conditions were coil rf power of 700 W, dc-bias voltage to substrate of 300 V, and gas pressure of 5 mTorr. As the Cl_2 concentration increased, the etch rate rapidly decreased and then remained constant. Although the chlorine radicals in the plasma increased due to increase of Cl_2 concentration, the etch rate decreased. This means that the vertical sputtering effect by the bombardment of Ar ions onto the substrate has more influence on the etch rate than the chemical effect by the surface reaction with the chlorine radicals. Therefore, it is conceivable that the etch mechanism of Ni films is mainly ion sputtering.

FESEM micrographs of Ni films etched at various Cl_2 concentrations were shown in Figure 2. When Ni films were etched by pure Ar, the redeposition occurred around the etched films. As the Cl_2 concentration increased, no redeposition around the etched patterns occurred and the sidewall slope of the etched films became slanted. The higher the Cl_2 concentration was, the more slanted the sidewall slope of the etched films became. The etched surfaces of the Ni films became smoother with increasing Cl_2 concentration because ion sputtering was reduced by the increase of Cl_2 gas and the chemical reaction of the films was enhanced. The high degree of anisotropic etching without the redeposition was obtained at 20 % Cl_2/Ar gas. This verifies the influence of physical bombardment by Ar ions on the etch characteristics such as the etch rate and the etch profile.

In order to attain more precise understanding of the etching mechanism, it is meaningful to inspect the etched surfaces of Ni thin films at different Cl_2 concentrations. Figure 3 showed the XPS full spectra of as-deposited Ni film and etched Ni films at 20 and 80 % Cl_2 concentrations. Bare Ni thin films without photoresist masks were used as the specimens for this analysis. The etched specimens were not rinsed so as to keep the etched surface in as-etched state. Through a comparison of the full spectra, Cl 2p peaks were observed on all film surfaces etched using Cl_2/Ar mix gas. This indicates the existence of chlorine compounds on the etched surfaces. Figure 4

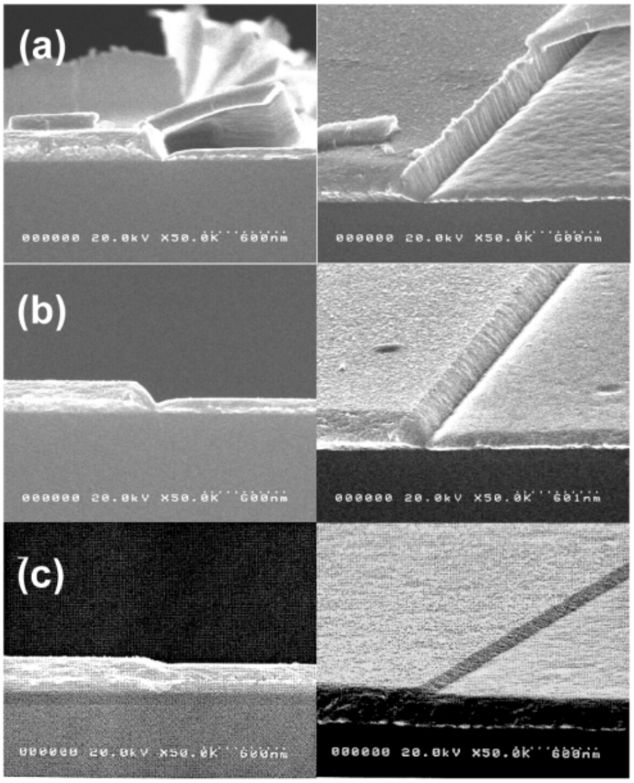

Figure 2. FESEM micrographs of etched Ni thin films at various Cl_2 concentrations. (a) pure Ar, (b) 20 % Cl_2/Ar, and (c) 60 % Cl_2/Ar, coil rf power of 700 W, dc-bias voltage of 300 V, gas pressure of 5 mTorr.

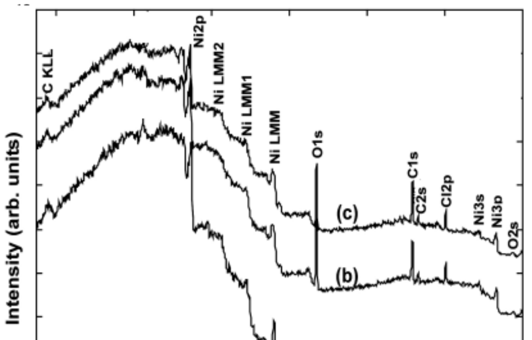

Figure 3. XPS spectra of (a) as-deposited Ni film, and etched Ni films at (b) 20 % Cl_2/Ar, and (c) 80 % Cl_2/Ar, coil rf power of 700 W, dc-bias voltage of 300 V, gas pressure of 5 mTorr.

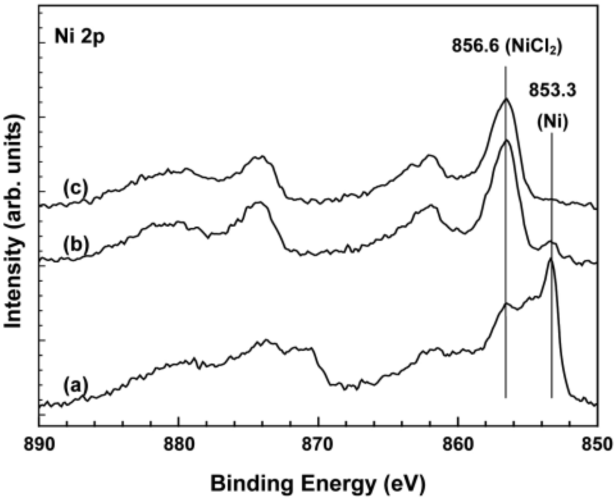

Figure 4. XPS narrow scans of Ni 2p spectra for (a) as-deposited Ni film, and etched Ni films at (b) 20 % Cl_2/Ar, and (c) 80 % Cl_2/Ar, coil rf power of 700 W, dc-bias voltage of 300 V, gas pressure of 5 mTorr.

showed narrow scans of the Ni 2p peaks. A single chemical state of nickel with small amount of nickel compounds was detected on the surface of as-deposited specimen, corresponding to nickel metal with a binding energy (Ni $2p_{3/2}$) of 853.3 eV. After etching at 20 % Cl_2 concentration, two chemical states of nickel, which showed a small shoulder at 853.3 eV (Ni) and a major feature at 856.6 eV, were detected on the etched surface. On the other hand, in the case of 80 % Cl_2 concentration, only one peak (binding energy of 856.6 eV) was observed on the etched Ni surface. According to data found in the literature, the binding energy for $NiCl_2$ is in the range of 856.3 ~ 856.7 eV. These results presented the existence of etch byproduct (mainly $NiCl_2$) by chemical reaction of the films regardless of gas concentrations. The reason why metal peak of 853.3 eV was observed at 20 % Cl_2 concentration was due to the fact that the plasma with 20 % Cl_2 concentration has more ion sputtering effect so that the amount of Cl radicals was not enough to react with all sputtered Ni atom. Since the plasma with 80 % Cl_2 concentration, however, has chemical component of Cl radicals as well as ion sputtering of Ar ions, Ni metal peak at etched film surface was not detected. This conclusion was confirmed by the fact that Ni metal peak was only detected on film surface etched at 20 % Cl_2 concentration.

The effects of etch parameters containing coil rf power, dc-bias voltage, and gas pressure on the etch rate and etch profile were also investigated. The standard etch conditions were 20 % Cl_2/80 % Ar, 700 W coil rf power, 300 V dc-bias voltage, and 5 mTorr gas pressure. In order to examine the influence of etch parameters, one parameter was varied for each case while the other parameters including gas concentration were kept the same. As the coil rf power increased from 500 to 900 W, the etch rates increased substantially and the sidewall slopes of the etched films became steeper, as shown in Figure 5. These etch results are attributed to the increase of Ar ions and Cl radicals by an increase of the plasma density at

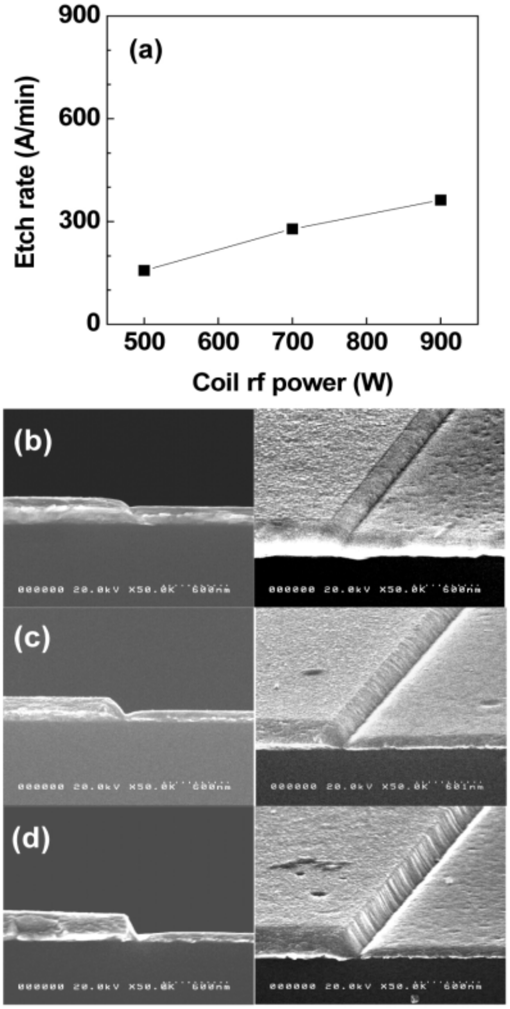

Figure 5. Etch rate (a) and FESEM micrographs of Ni thin films etched at various coil rf powers, (b) 500 W, (c) 700 W, and (d) 900 W, 20 % Cl_2/Ar gas, dc-bias voltage of 300 V, gas pressure of 5 mTorr.

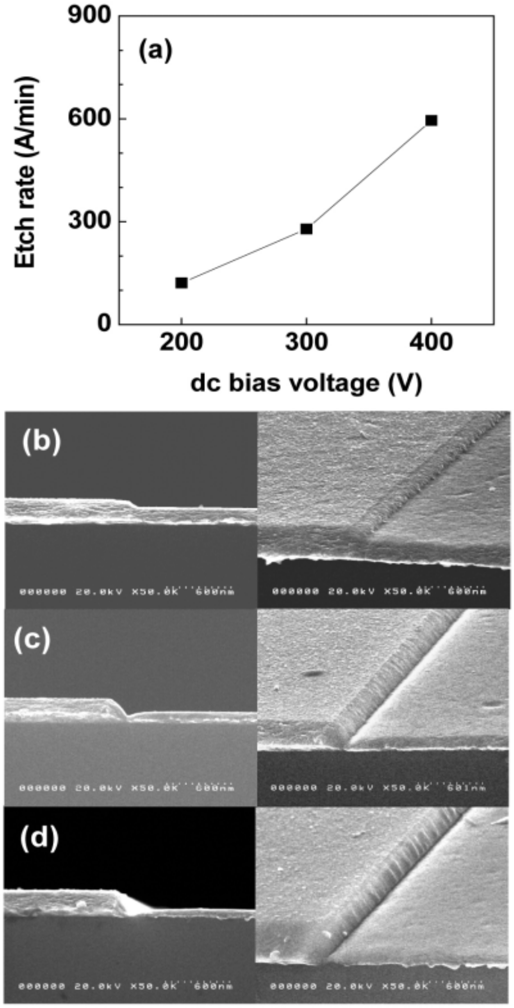

Figure 6. Etch rate (a) and FESEM micrographs of Ni thin films etched at various dc-bias voltages, (b) 200 V, (c) 300 V, and (d) 400 V, 20 % Cl_2/Ar gas, coil rf power of 700 W, gas pressure of 5 mTorr.

high coil rf power. Both ion bombardment and chemical reaction were enhanced due to the increase of Ar ions and Cl radicals at high coil rf power. For the case of dc-bias voltage variation, the same tendencies as coil rf power were obtained. The etch rates increased and etch profiles were improved for an increase of dc-bias voltage from 200 to 400 V (Figure 6). This results from the increased bombardment energy of ions at high dc-bias voltage. It is clear from the variations of coil rf power and dc-bias voltage that ion bombardment onto the films is the crucial factor in determining the etch rate and etch profile. High coil rf power and high dc-bias voltage resulted in a fast etch rate and steep etch profile. Figure 7 showed the effect of gas pressure on the etch rate and etch profile. As the gas pressure increased from 1 mTorr to 10 mTorr, the etch rate remained almost constant whereas the etch profile at low gas pressure became clean and steep. Because the mean free path of ions at low gas pressure is longer than that at high gas pressure, the vertical sputtering effect is enhanced. By utilizing the results of these systematic studies of the etch parameters, a high degree of anisotropy in the etch profile of Ni films could be achieved without any redepositions or etch residues.

Conclusion

Dry etching of Ni thin films patterned with a photoresist mask was carried out in an inductively coupled plasma of Cl_2/Ar gas. As the Cl_2 concentration increased, the etch rate and the degree of anisotropy decreased. These results imply that the main etch mechanism is ion sputtering onto the films. It was demonstrated from XPS analyses that Ni films reacted with chlorine radicals to form $NiCl_2$ compounds in a Cl_2/Ar plasma. In addition, more ion

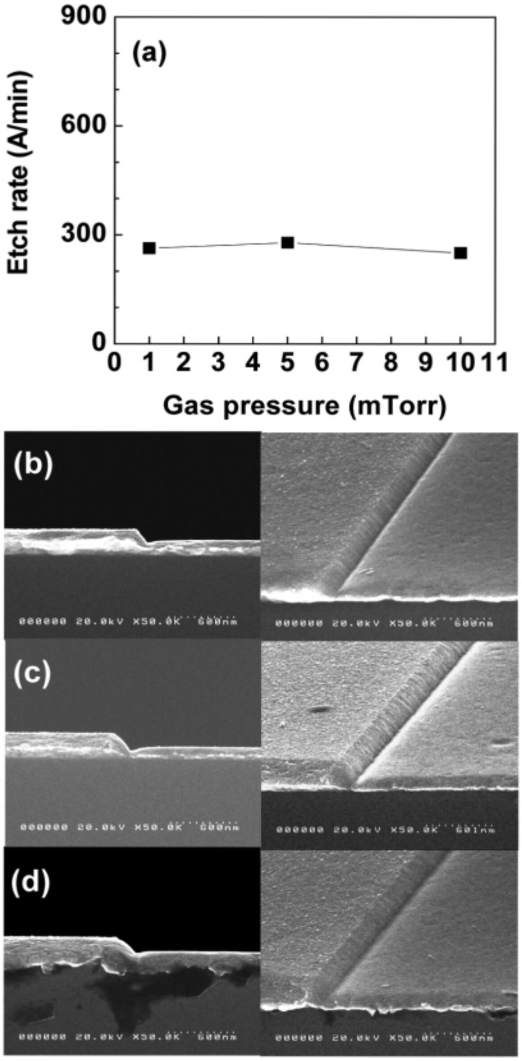

Figure 7. Etch rate (a) and FESEM micrographs of Ni thin films etched at various gas pressures, (b) 1 mTorr, (c) 5 mTorr, and (d) 10 mTorr, 20 % Cl_2/Ar gas, coil rf power of 700 W, dc-bias voltage of 300 V.

sputtering effect was proved at lower Cl_2 concentration by the XPS analysis. The etch rate and the sidewall slope of the etched films increased with increasing coil rf power and dc-bias voltage. By varying gas pressure, little change in the etch rate was observed and good etch profile was obtained at low gas pressure. Based on the above results, it could be concluded that the etching of Ni thin films is governed by ion sputtering along with chemical assistance.

Acknowledgments

This work was supported by Samsung Advanced Institute of Technology.

References

1. A. Takashi, G. H. Youn, and E. Masayoshi, *J. Vac. Sci. Technol. B*, **21**, 2159 (2003).
2. K. B. Jung, E. S. Lambers, J. R. Childress, S. J. Pearton, M. Jenson, and A. T. Hurst Jr., *Appl. Phys. Lett.*, **71**, 1255 (1997).
3. K. B. Jung, J. Hong, J. Cho, J. A. Caballero, J. R. Childress, S. J. Pearton, M. Jenson, and A. T. Hurst Jr., *Appl. Surf. Sci.*, **138**, 111 (1999).
4. I. G. Baek, M. S. Lee, S. Seo, M. J. Lee, D. H. Seo, D.-S. Suh, J. C. Park, S. O. Park, H. S. Kim, I. K. Yoo, U.-In. Chung, and J. T. Moon, in Proc. *The 2004 IEEE International Electron Devices Meeting*, pp. 587-590, San Francisco, USA (2004).
5. I. G. Baek, D. C. Kim, M. J. Lee, H.-J. Kim, E. K. Yim, M. S. Lee, J. E. Lee, S. E. Ahn, S. Seo, J. H. Lee, J. C. Park, Y. K. Cha, S. O. Park, H. S. Kim, I. K. Yoo, U-In Chung, J. T. Moon, and B. I. Ryu, in Proc. *The 2005 IEEE International Electron Devices Meeting*, pp. 750-753, Washington, USA (2005).
6. S. Seo, M. J. Lee, D. H. Seo, E. J. Jeoung, D. S. Suh, Y. S. Joung, I. K. Yoo, I. R. Hwang, S. H. Kim, I. S. Byun, J. S. Kim, J. S. Choi, and B. H. Park, *Appl. Phys. Lett.*, **85**, 5655 (2004).
7. J. F. Gibbons and W. E. Beadle, *Solid-State Electron*, **7**, 785 (1964).
8. M. J. Vasile and C. J. Mogab, *J. Vac. Sci. Technol. A*, **4**, 1841 (1986).
9. K. B. Jung, E. S. Lambers, J. R. Childress, S. J. Pearton, M. Jenson, and A. T. Hurst Jr., *J. Electrochem. Soc.*, **145**, 4025 (1998).
10. I. H. Park, J. W. Lee, and C. W. Chung, KIEC, **11**, 509 (2005).